

The design of closed loop type BPF with two attenuation poles at the upper side of passband

Dal Ahn*, Min-Ho Chung*, Chul-Soo Kim*, Yang-Kyun Shin**, Young-Chae Jeong***

* Dept. of Electronics, SoonChunHyang Univ., Korea

** Haitai Electronics Co. LTD., Korea

*** Samsung Electronic Co. LTD., Korea

Abstract

In this paper, a new design method of BPF which has two attenuation poles at the upper side of passband, using closed loop type resonator and perturbation elements, is presented. The closed loop resonator based on TEM mode is analyzed by the network analytical method, and the effect of perturbation element is investigated. The advantage of this method is the high attenuation at the upper side of passband because of two attenuation poles. To prove usefulness of the proposed synthesis method, it compares the simulation data with the experimental result measured by the vector network analyzer(VNA). There is good agreement between them.

1. Introduction

The modern communication systems such as cellular phone system, cordless phone system and global positioning system, require high performance BPFs. When we design those systems, filters which have very high rejection characteristic of specific frequency band and very small size are needed. In this case, the BPF design is very difficult^[1]. In order to design above filters, the design method of BPF using ring resonator had been presented in many papers^{[2][3]}. However there are many problems and difficulties in realization because the analysis and design of ring resonator and filter are performed by field theory on the basis of non-TEM mode.

On the contrary, we applied the network analytical method on the basis of TEM mode in analysis of closed loop resonator which is general form of ring resonator^[4]. The merits of closed loop resonator have two attenuation poles, high-Q value and small size. The perturbation elements are used to control of attenuation pole. Therefore, a small BPF can be designed very easily with this method, and attenuation slope at the upper side of passband has very high value because of attenuation pole.

To prove that our design method is useful, we designed, realized and measured the 2-pole and 4-pole BPF through our design method. We will show good agreement between the predicted performances of designed BPFs and the measured performances of fabricated BPFs.

2. Design Method and Theory

Fig. 1 shows the structure of 2-pole BPF which consists of closed loop resonator with perturbation elements.

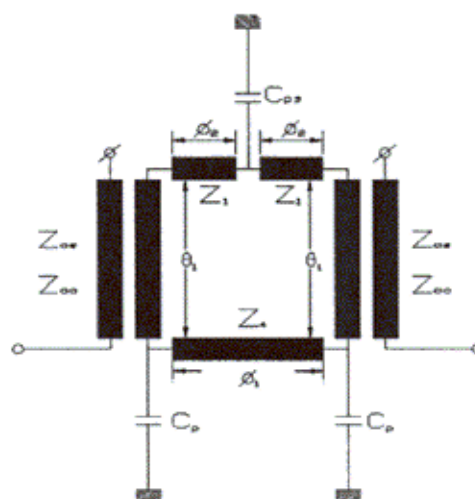
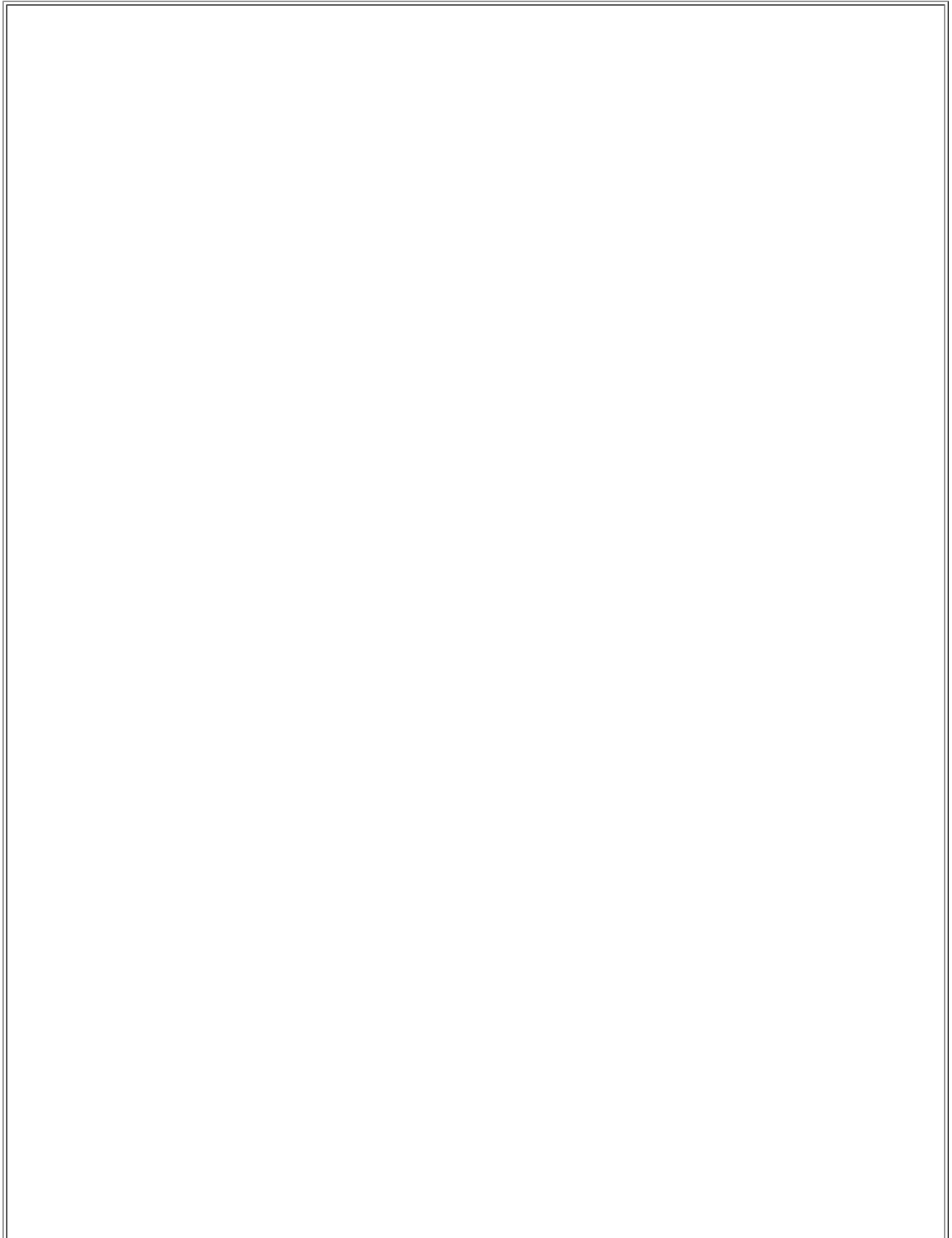


Fig. 1 The structure of 2-pole BPF

Using the equivalent circuit of coupled lines with one port is open, Fig. 1 can be expressed as shown in Fig. 2^[5].

[다음](#)



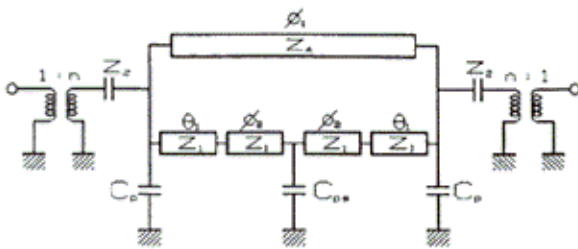


Fig. 2 The equivalent circuit of 2-pole BPF shown in Fig. 1

where

$$n = \frac{Z_{oe} + Z_{oo}}{Z_{oe} - Z_{oo}} \quad (1)$$

$$Z_1 = \frac{Z_{oe} + Z_{oo}}{2} \quad (2)$$

$$Z_2 = Z_1(n^2 - 1) \quad (3)$$

Fig. 2 can be converted to Fig. 3 using π -type equivalent circuit of transmission line and π -T transformation.

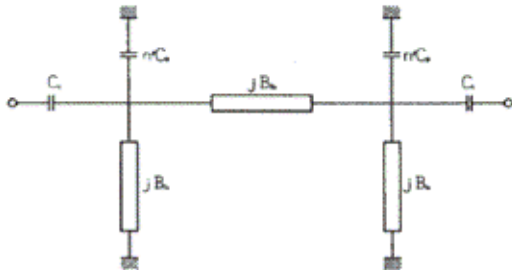


Fig. 3 The simplified π -type equivalent circuit of 2-pole BPF

C_1 , jB_a , and jB_b in Fig.3 are expressed as eq. (4) ~ (6).

$$j\omega C_1 = j \frac{n^2}{Z_2} \tan \theta_1 \quad (6)$$

Fig.4 shows the structure of 4-pole BPF which consists of two closed loop resonators and perturbation elements.

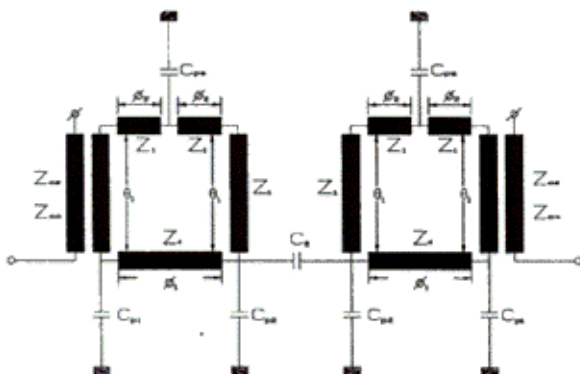


Fig. 4 The structure of 4-pole BPF

In the same method, Fig. 4 can be expressed as shown in Fig. 5.

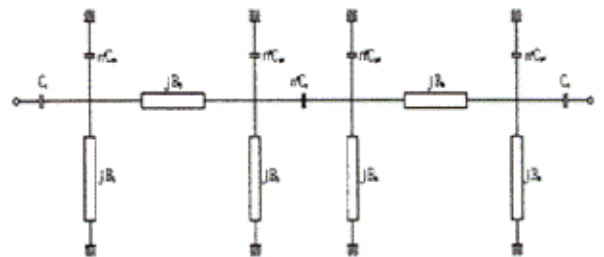


Fig. 5 The simplified π -type equivalent circuit of 4-pole BPF

The equivalent circuit of $2n$ -pole BPF with J-inverters is shown in Fig. 6.

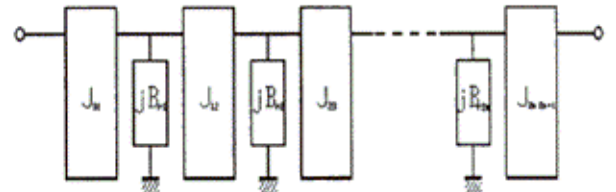


Fig. 6 The equivalent circuit of $2n$ -pole BPF with J-inverters

As shown in Fig. 3 and Fig. 5, the equivalent circuit of closed loop resonators with perturbation elements must be equivalent with Fig. 6 to have the characteristic of BPF. Eq. (7)~(19) are derived from the equivalence between the circuit in Fig.3, Fig. 5 and Fig. 6.

$$jB_{r1} = j(B_a + B_b) + j\omega C_{t1} \quad (7)$$

$$jB_j = j(B_a + B_b) + j\omega C_j \quad (8)$$

$$jB_{r2n} = j(B_a + B_b) + j\omega C_{t2n} \quad (9)$$

$$J_{01} = \sqrt{\frac{Y_0 B_{r1}(\omega_2)}{\omega_1 g_0 g_1}} \quad (10)$$

$$J_{j,j+1} = \sqrt{\frac{B_{rj}(\omega_2) B_{rj+1}(\omega_2)}{(\omega_1 g_j)(\omega_1 g_{j+1})}} \quad (11)$$

$$J_{2n,2n+1} = \sqrt{\frac{Y_0 B_{r2n}}{(\omega_1 g_{2n})(\omega_1 g_{2n+1})}} \quad (12)$$

where

$$C_{t1} = (C_{p1} n^2 + C_1^e) \quad (13)$$

$$C_j = n^2 (C_{pj} + C_j) \quad (14)$$

$$C_{t2n} = (C_{p2n} n^2 + C_{2n+1}^e) \quad (15)$$



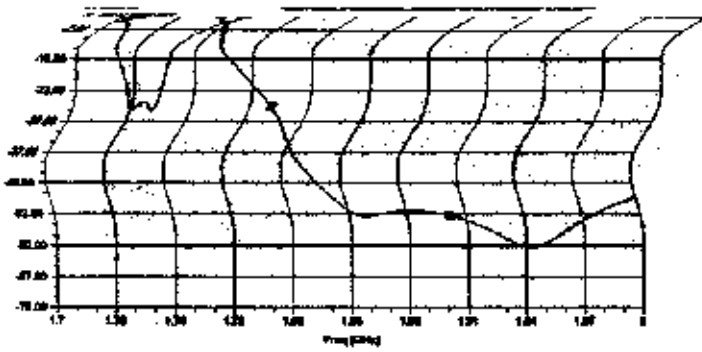


Fig. 7 The simulated result of 2-pole BPF

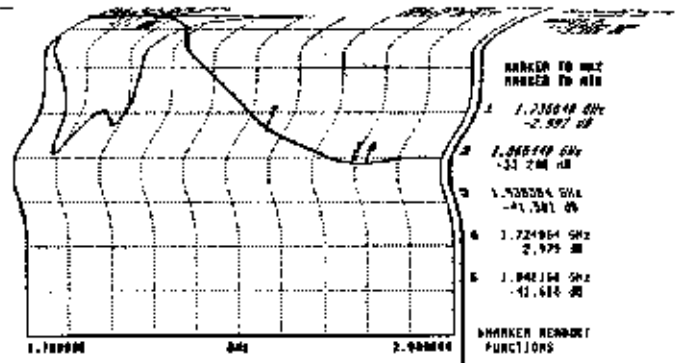


Fig. 9 (a) The measured performance of 2-pole BPF

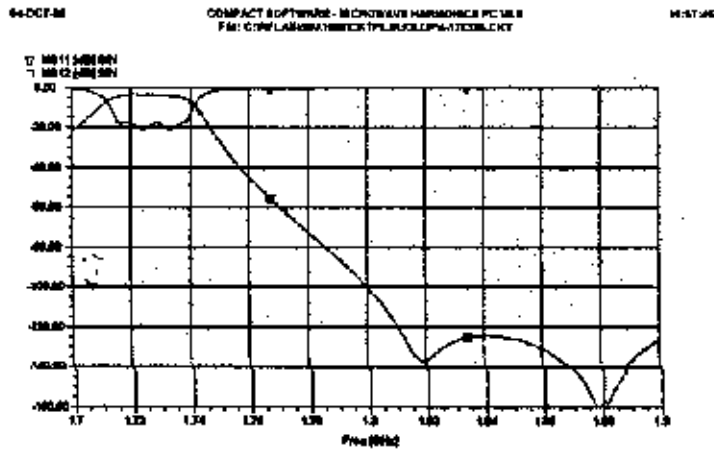


Fig. 8 The simulated result of 4-pole BPF

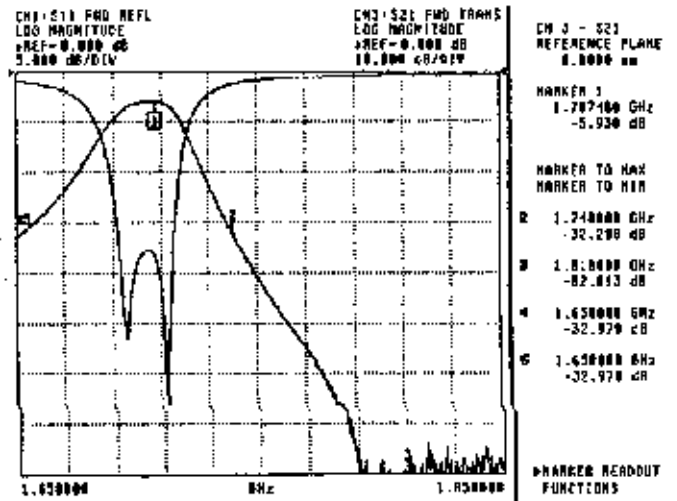


Fig. 9 (b) The measured performance of 4-pole BPF